

# Effect of a heterogeneous distribution of particles on the formation of banded grain structure in wrought Alloy 718

Sébastien Coste, Eric Andrieu and Julitte Huez

CIRIMAT—UMR CNRS 5085, Laboratoire Interface et Matériaux, ENSIACET 118 route de Narbonne, F-31077 Toulouse cedex 4, France

Aubert & Duval Fortech, Service Métallurgie, 75 Boulevard de la libération, F-09102 Pamiers cedex, France

Received 8 September 2003; revised 20 December 2004; accepted 22 December 2004.

Available online 26 February 2005.

## Abstract

Alloy 718 is known to be sensitive to interdendritic segregation formed during ingot solidification. The occurrence of banded grain structures under heat treating conditions close to 1000 °C related to interdendritic segregation is often reported. In order to have a better understanding of this microstructural evolution, an extensive experimental program has been carried out. Consequently, a model taking into account the selective dissolution of  $\delta$ -phase ( $\text{Ni}_3\text{Nb}$ ) is proposed. A grain growth simulation by Monte-Carlo method is then used to illustrate the grain structure evolution in a banded particle distribution. By comparing experimental data and computer simulation, the relationship between the Monte-Carlo step and the real time is assessed and the range of parameters when heterogeneous microstructures appear is specified.

**Keywords:** Monte-Carlo; Grain growth; Alloy 718; Heterogeneous microstructure

1. Introduction
  2. Monte-Carlo method
  3. Choice of initial conditions
  4. Case of randomly distributed particles
    - 4.1. Influence of temperature
    - 4.2. Influence of  $\delta$ -phase fraction
    - 4.3. Discussion
  5. Relationship between real time and MCS
  6. Banded distribution of particles
  7. Conclusions
- Acknowledgements  
References

## 1. Introduction

The nickel base superalloy 718 is widely used for high temperature applications as in gas turbine discs and other rotating parts. Since its mechanical properties strongly depend on its microstructure, every step of the thermomechanical processing has to be well controlled. In order to reach this objective, an accurate knowledge of the microstructural evolution of Alloy 718 in relation to process parameters and a suitable model is necessary to optimize the processing route. However, for this alloy prediction of the microstructural evolution is difficult due to its high

sensitivity to dendritic segregations of elements with low diffusivity. Indeed, the solubility temperature of  $\delta$ -phase precipitates is located in the range of the process window for hot deformation. The typical forging temperature is near 1000 °C and can reach about 1050 °C due to adiabatic heating. Then, the effect of varying phase fractions can significantly affect the microstructure and mechanical properties during and after the deformation process.

The present study is part of an extensive work devoted to the determination of microstructural evolution laws in the nickel base superalloy 718. There, a Monte-Carlo simulation has been developed to quantify the influence of dendritic segregations on the microstructural evolution. The first part of this work deals with a study of grain growth with a random distribution of the particles. The first step of the modelling allowed to assess the influence of the temperature of heat treatment and the influence of the  $\delta$ -phase fraction on the grain growth. Furthermore, determination of a relationship between the Monte-Carlo step (MCS) and the real time is established, making it easier to compare simulated microstructure and experimental data. The second part of this work is devoted to the study of the effect of a heterogeneous particle spatial distribution on grain growth. This  $\delta$ -phase distribution, which is more realistic, allows to specify the range of parameters when heterogeneous microstructures appear.

## 2. Monte-Carlo method

The Monte-Carlo simulations of grain growth were performed in 400×400 triangular matrices. The orientation number  $Q_k$  of a given lattice site  $k$  ranged from 1 to  $Q_{\max}$ , with  $Q_{\max}=130$  in the present simulations. Each lattice site  $k$  is surrounded by six sites  $Q_N(k,j)$  with  $j=1-6$ . A grain is defined as an aggregate of lattice points with an identical  $Q$  number (Fig. 1).

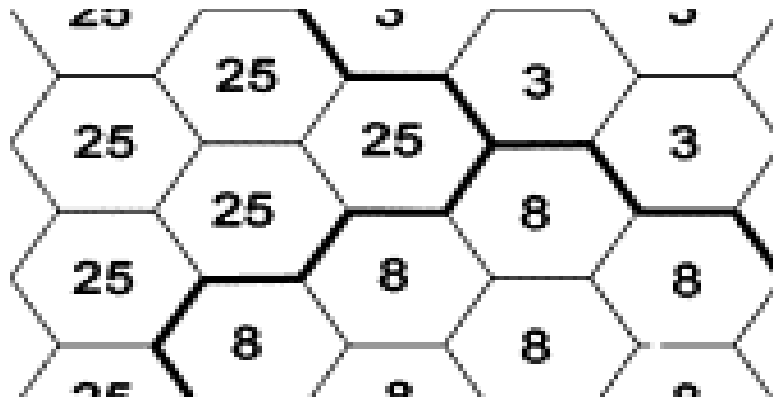


Fig. 1. Hexagonal lattice used in the Monte-Carlo simulations (orientation numbers).

A grain boundary is defined as the interface between two lattice points of different  $Q$  numbers. A special orientation number, 0, was assigned to the lattice sites where the second phase particles were embedded. The energy of the system is given by Eq. (1).  $\gamma$  is the linear grain boundary energy and  $\delta(Q_k, Q_{N(k,j)})$  the Kronecker delta function.

$$E = -\gamma \sum_k \sum_{j=1}^6 [\delta(Q_k, Q_{N(k,j)}) - 1]. \quad (1)$$

The change of grain boundary energy accompanying reorientation is a driving force for grain boundary migration. The Monte-Carlo simulation of grain growth can be performed by the Metropolis algorithm. The procedure of the simulation is as follows:

- One lattice site  $k$  is randomly selected.

- A new orientation of the lattice is generated. Switching the orientation number of second phase particles is totally prohibited.
- The change in energy,  $\Delta E$ , associated with the change of spin variables is calculated.
- The reorientation trial is accepted, if  $\Delta E$  is less than or equal to zero. If  $\Delta E$  is greater than zero, the reorientation is related to a Boltzmann probability  $p$ :

$$p = \exp\left(-\frac{\Delta E}{kT}\right). \quad (2)$$

The time scale of the simulation is the Monte-Carlo step. One MCS is related to  $N$  re-orientation attempts, where  $N$  is the number of lattice sites (160,000).

### 3. Choice of initial conditions

The typical chemical composition of Alloy 718 is given in [Table 1](#). It is a nickel base alloy with a high content of iron, chromium and niobium.

Table 1.

Nominal chemical composition of Alloy 718 (wt.%)

C	0.02
Cr	17.89
Ni	Balance
Fe	17.35
Mo	2.97
Nb	5.40
Ti	1.07
Al	0.46

In order to have a relevance interest, Monte-Carlo simulations are performed with initial conditions based on microstructural observations. In a previous work [[1](#)], the influence of the niobium concentration on the  $\delta$ -phase behavior has been studied. Local variations of niobium content lead to a disparity in the local volume fraction of precipitates. It was observed, that these heterogeneities of distribution in terms of  $\delta$ -phase fraction can significantly influence the local evolution of the microstructure. This effect highlights the role of the  $\delta$ -phase in the control of the grain boundary mobility by Zener pinning. Furthermore, these observations have permitted to obtain the range of the  $\delta$ -phase fraction for each heat treating condition. [Fig. 2](#) shows the initial microstructure used for computer simulations.

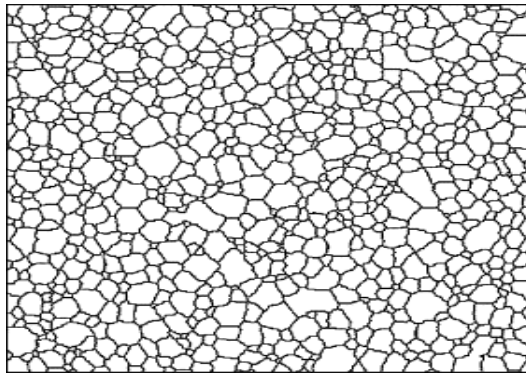


Fig. 2. Initial microstructure used in the simulation.

Four hundred hexagons in width represent  $400 \mu\text{m}$ . The unit area for one hexagon is  $0.866 \mu\text{m}^2$  and one particle is represented by one site and is randomly dispersed. With these conditions the particle radius is  $0.525 \mu\text{m}$ , which is close to the observed size [2]. The initial grain size is  $20 \mu\text{m}$  and the lattice represents about 800 grains. The initial distribution of grain size is a log-normal distribution as shown in Fig. 3.

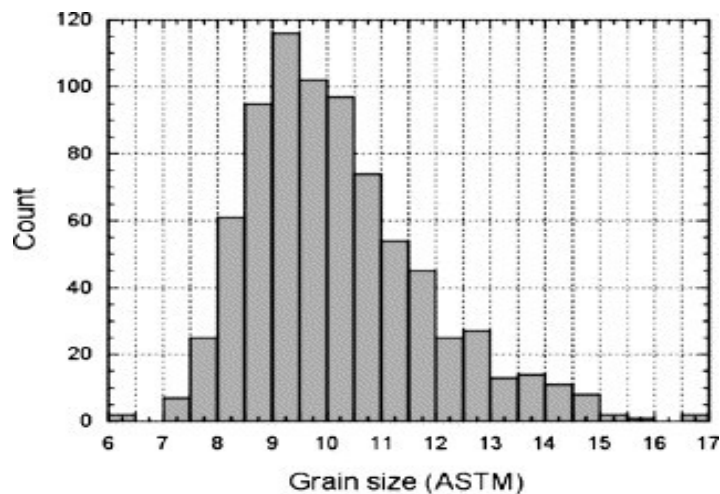


Fig. 3. Initial distribution of grain size.

This method was used to simulate the grain growth with second phase particles. There was neither growth nor dissolution of the second phase particles. This initial microstructure allowed us to study the influence of several parameters on the grain growth. Grain growth simulations for several temperatures ranging from  $990$  to  $1040^\circ\text{C}$  were performed. The particle area fractions range from  $0$  to  $10\%$  and the maximum MCS is equal to  $115,200$ .

## 4. Case of randomly distributed particles

### 4.1. Influence of temperature

Grain growth was simulated for two heat treating conditions ( $900$  and  $1040^\circ\text{C}$ ) and with two volume fractions of precipitates ( $0.5$  and  $2\%$ ). The results of the simulations are presented in Fig. 4. It is worth noting that for a given volume fraction of precipitates, the grain growth kinetics associated with the two heat treating conditions are not quite different but, when the fraction  $f$  increases from  $0.5$  to  $2\%$ , the grain growth kinetics slows down. Thus, the first order effect on the

grain growth kinetic seems to be due to the precipitate volume fraction.

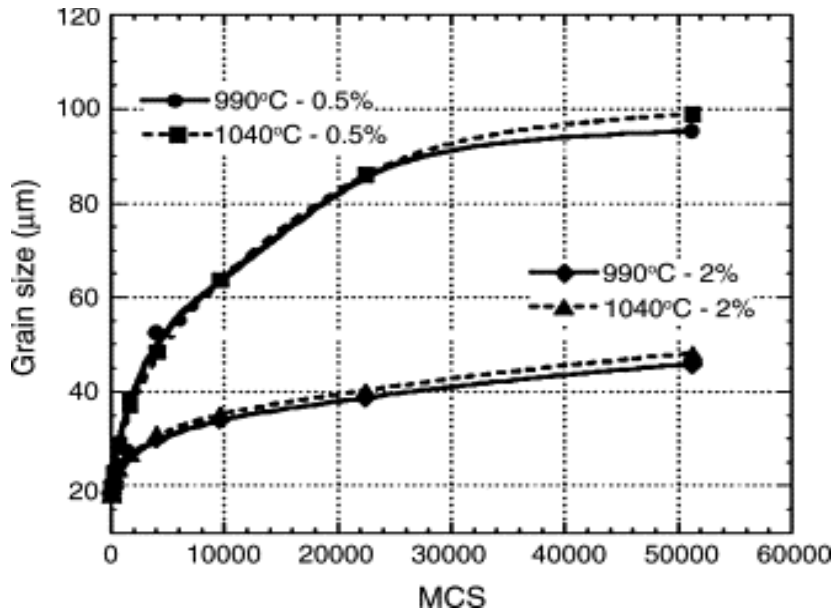


Fig. 4. Grain size evolution vs. MCS for two heat treatment temperatures (990 and 1040 ° C) with two different precipitate fractions (0.5 and 2%).

#### 4.2. Influence of $\delta$ -phase fraction

Grain growth simulations with a volume fraction of the  $\delta$ -phase  $f$  varying from 0 to 10% for a heat treatment at 1040 ° C are reported in Fig. 5. When  $f$  is greater than 4%, grain growth is limited. When  $f$  is less than 0.2%, little effects on the grain growth are observed. Between these two volume fractions of the  $\delta$ -phase, the grain size increases up to a limit. The limit grain size increases when the precipitate fraction decreases. The  $\delta$ -phase allows to control the microstructural evolution by pinning grain boundaries.

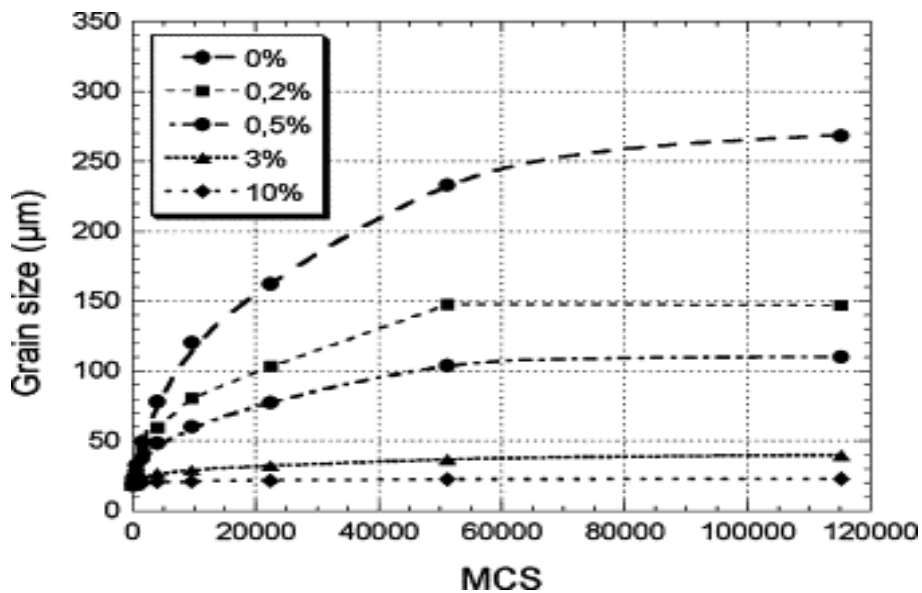


Fig. 5. Grain size evolution vs. MCS for heat treatments at 1040 ° C with precipitate fractions ranged from 0 to 10%.

### 4.3. Discussion

It is possible to compare simulation results of limit grain size with the limit grain size obtained by a Zener model. The Zener model refers to the inhibition effect of second phase particles on grain growth in polycrystalline materials. It was revisited [3], [4] and [5] and written in 2-D to obtain a relationship between the pinned grain size  $R_{\text{limit}}$ , the second phase particle size  $r$  and the fraction of precipitates  $f$ :

$$\frac{R_{\text{limit}}}{r} = kf^{-0.5}, \quad (3)$$

where  $k$  is a constant. By plotting (Fig. 6) the logarithm of the ratio  $R_{\text{limit}}/r$  versus the logarithm of  $f$ , a linear relation is found:

$$R_{\text{limit}} = r \frac{14 \pm 2}{f^{0.49 \pm 0.02}}. \quad (4)$$

This result agrees well with that of other authors [6].

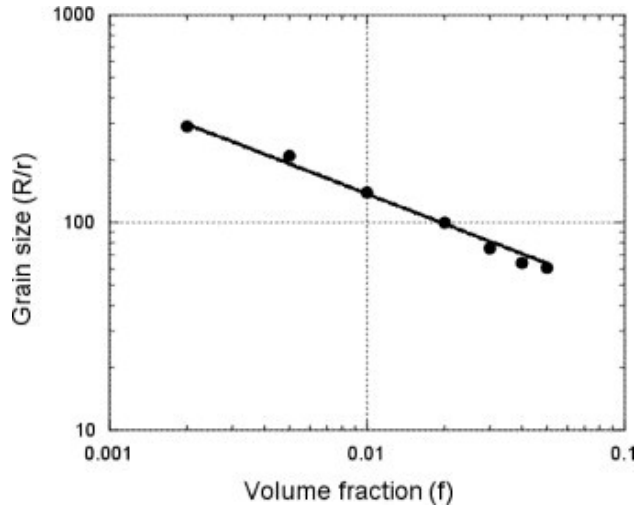


Fig. 6. Logarithm of the ratio between the grain size,  $R$ , and the radius of precipitates,  $r$ , vs. the logarithm of the particle fraction,  $f$ .

Fig. 7 shows the grain radius distribution by plotting the number of grains versus the logarithm of the normalized grain radius,  $R$  on the mean  $R$ , for several times of simulation. A log-normal distribution is obtained and is found to be independent of both time and particle concentration. These results are representative of normal kinetics of grain growth [7].

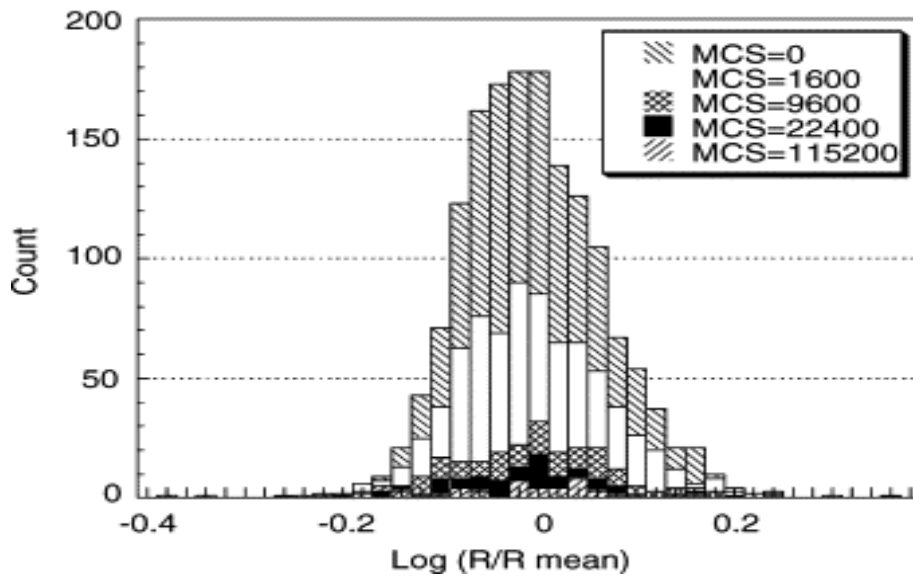


Fig. 7. Normalized grain size distribution of pinned structure.

## 5. Relationship between real time and MCS

Before using computer simulations in practical industrial applications, a link between the MCS and the real time must be established. For this purpose, experimental data and calculations have been compared. The main problems remain in the non-uniformity of the  $\delta$ -phase fraction in real materials [1] and the sensitivity of the microstructural evolution to dendritic segregations. To avoid these problems, the influence of the  $\delta$ -phase on the grain growth is minimized. Fig. 8 represents experimental data.

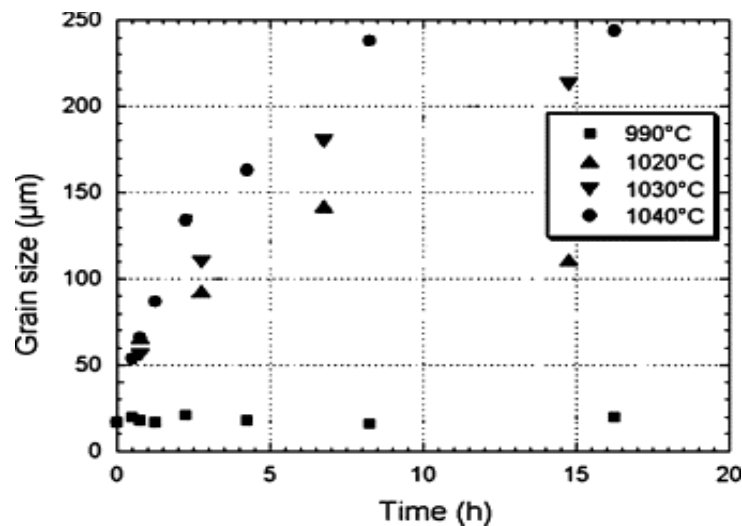


Fig. 8. Experimental grain size evolution vs. heat treatment time.

At 990 ° C, grain growth is not evidenced. At 1040 ° C, precipitates are dissolved and the grain growth follows a classical law of growth. Between these two extreme cases, the microstructural evolution becomes more sensitive to dendritic segregation as the temperature decreases. For example, in Fig. 8 the grain growth of samples heat treated at 1020 ° C do not follow a global trend. This phenomenon is probably due to the inability to represent a bimodal grain size distribution by a mean grain size.

The relationship between the MCS and the real time is obtained by finding the correspondence

between them for a given grain size. For example, at 1040 ° C, the experimental grain size is 140 μ m after 4 h of treatment and by simulation, 140 μ m is obtained for 140,000 MCS. These comparisons are reported by plotting in Fig. 9 the real time versus the obtained MCS.

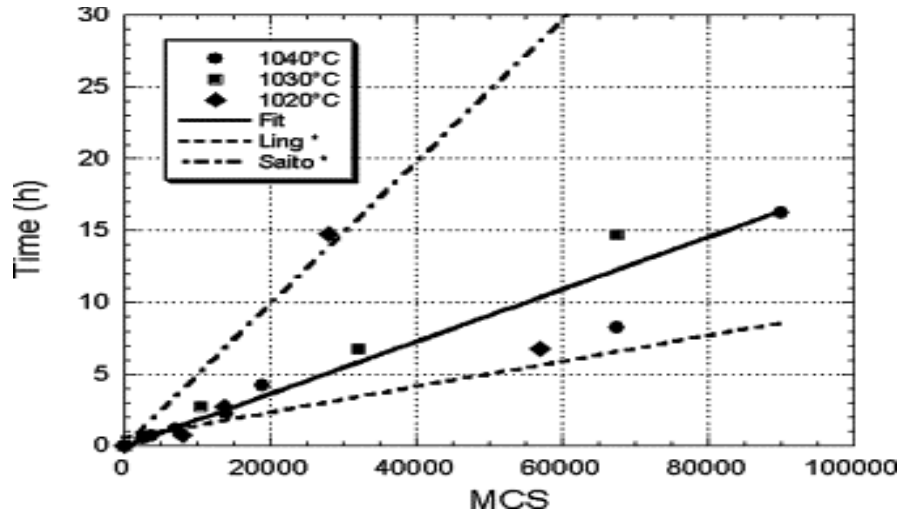


Fig. 9. Real time vs. MCS.

The relationship between Monte-Carlo step and real time seems to be linear for heat treatment duration except for grain growth at 1020 ° C where results are more dispersed. This discrepancy is due to pinning. At this temperature, precipitates have a great influence on the grain growth rate. By using upper temperatures, the real time is directly proportional to the MCS:

$$\text{time (min)} = 0.65\text{MCS}. \quad (5)$$

A similar type of experimental relationship has been found by Ling and Anderson [8] with different coefficients:

$$\text{time (min)} = 2044 + 0.32\text{MCS}. \quad (6)$$

This discrepancy can be explained by the fact that the relationship formula may depend on the lattice parameter or others conditions. Saito [9] proposed an idea based on diffusion considerations, with  $d$  the lattice parameter,  $Q$  the number of orientation and  $D$  the macroscopic diffusion coefficient. However, the main problem is to determine the apparent diffusion coefficient which controls grain growth in the present study. This formula gives a linear relationship, too, and is used to compare experimental and simulated grain growth kinetics (Fig. 10):

$$1\text{MCS} = \frac{d^2}{6DQ}. \quad (7)$$

As shown in Fig. 10, a good agreement between experimental and simulated grain growth kinetics is found for several heat treating conditions. However, it is worth noting that the discrepancy between experimental results and computer simulation evidenced the effect of the heterogeneity of  $\delta$ -phase particle distribution due to dendritic segregations at 1020 ° C. This point is addressed hereafter.



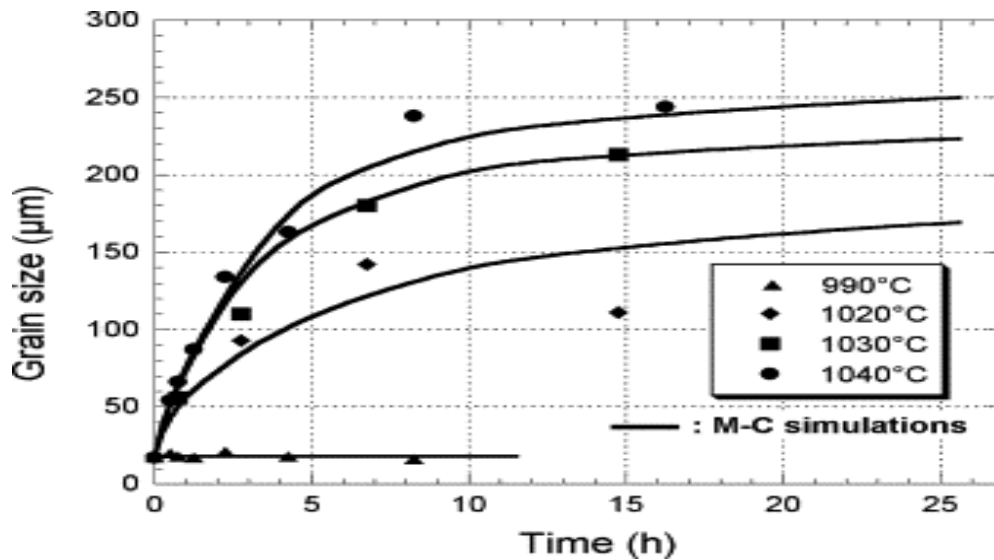


Fig. 10. Comparison between experimental and simulated grain growth kinetics.

## 6. Banded distribution of particles

In this section, the effect of non-uniform spatial distribution of the particles on grain growth is studied. This distribution is more realistic and should allow to specify the range of parameters when heterogeneous microstructures appear. It is well known that the microstructural evolution in Alloy 718 is strongly dependent on dendritic segregation during heat treatment in the range of the solubility temperature of  $\delta$ -phase. This dendritic segregation appears during ingot solidification. It is characterized by an interdendritic spacing which is about 200  $\mu$  m in the present case as illustrated in Fig. 11.

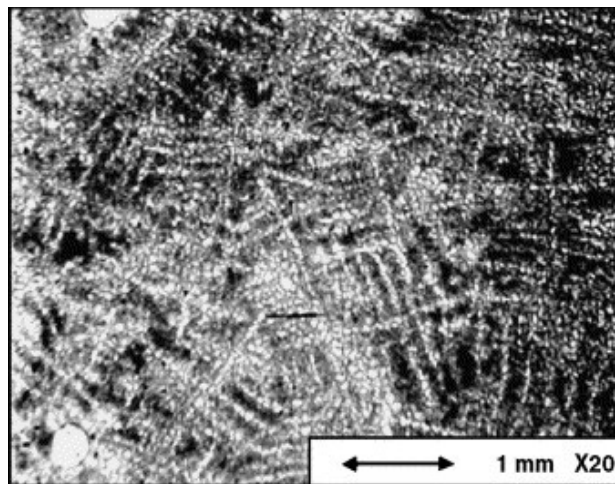


Fig. 11. Micrograph illustrating dendritic segregations (revealed by etching technique).

A re-homogenization treatment allows to decrease the difference in niobium content between interdendritic areas and dendritic cores down to 0.4 wt.%. Though smoothed by this heat treatment, such difference leads to a non-uniform spatial distribution of precipitates. Alternate bands of large and small grains observed after heat treatments (see SEM micrograph in Fig. 12a) are presumably related to banding distribution in the material and to the resulting banding of delta precipitate distribution. Such a microstructure has been simulated and the final step is presented in Fig. 12b. Both microstructures are comparable.

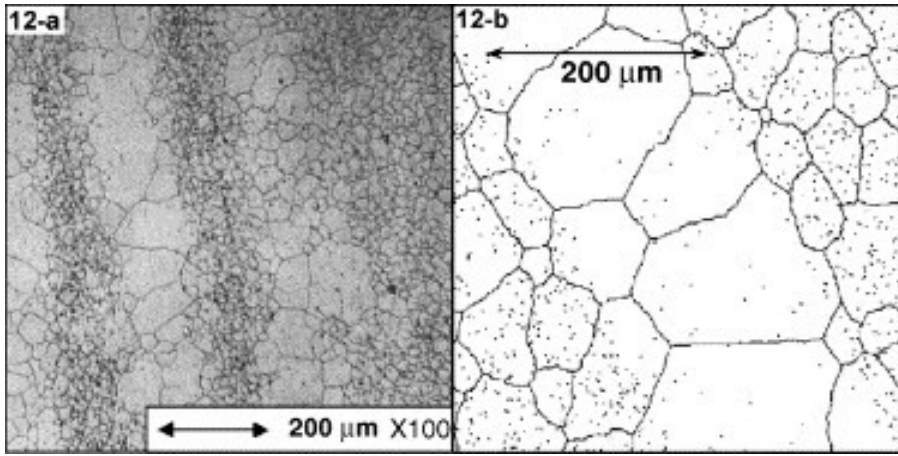


Fig. 12. (a) Micrograph showing a heterogeneous distribution of delta particles (black dots) and banded grain structure. (b) Final step of a microstructure obtained with an initial distribution of delta particles representative of (a).

In order to optimize process parameters it is important to know the real influence of this distribution on grain growth. Fig. 13 presents two sequences of microstructural evolution calculated for temperature respectively lower than 1000 °C and in between 1000 °C and the solvus temperature. In both cases, the sequence goes from the initial microstructure to the pinned state after 21 h of heat treatment. For a better visibility, particles are not represented in the pictures but are plotted on the simulated final microstructure shown in Fig. 12b. At temperatures less than or equal to 1000 °C there is a minor effect of the final particles distribution on the grain size distribution. For temperatures greater than 1000 °C, Fig. 13 shows clearly that a bimodal grain size distribution evolves. To quantify this heterogeneity and to assess the range of controlling parameters where it appears, a new index referred to as heterogeneity index is defined:

$$I_g = \frac{R_{\max}}{R_{\min}} \quad (8)$$

$R_{\max}$  is the average size for coarse and  $R_{\min}$  is the average size for fine grains.

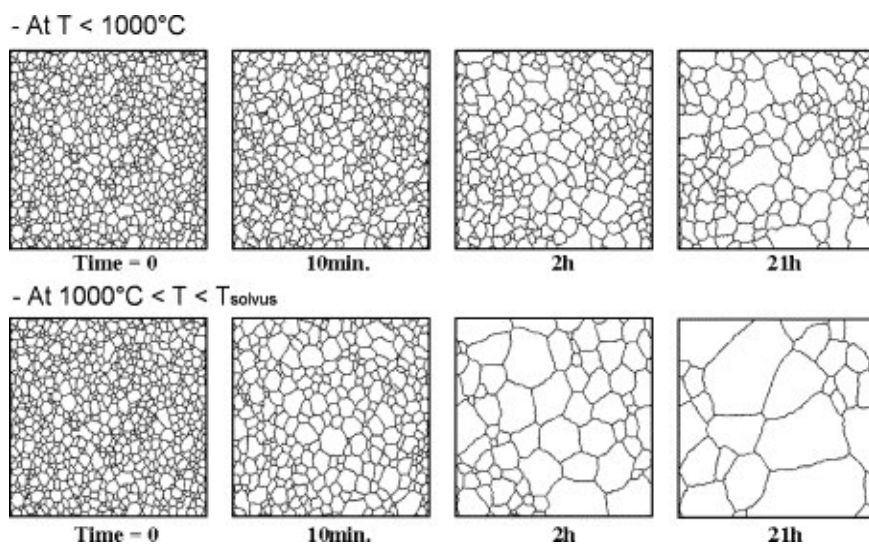


Fig. 13. Sequences showing the grain growth in a banded distribution of particles from the initial to a pinned state after 21 h under heat treating conditions at a temperature less than or greater than 1000 °C.

In practice, the grain size is given in ASTM numbers,

$$R^{ASTM} = -2.9542 - 3.3219 \log(A), \quad (9)$$

where  $A$  is the grain area in  $\text{mm}^2$ . In the following, the microstructure is considered as heterogeneous when  $R_{\text{max}}^{ASTM}/R_{\text{min}}^{ASTM} > 1.5$ , i.e.  $I_g > 1.68$ . By computer simulation, it is possible to assess  $I_g$  for any isothermal heat treating condition. It is then possible to draw an heterogeneity map (Fig. 14) by plotting iso-index lines in a temperature–time plane. This map underlines the boundary between homogeneous and heterogeneous microstructures however without consideration to the actual sizes. As illustrated above, the grain size distribution remains homogeneous at low temperature with an index lower than 1.3 even for the longest heat treatments considered. This is due to the fact that grain boundaries are strongly pinned to the particles. For the opposite reason, i.e. that grain boundaries easily overtake particles at high temperature, the grain size distribution remains also homogeneous for heat treating close to the  $\delta$  solvus temperature. At intermediate temperature, competition between pinning and grain boundary displacement is such that a two-fold grain size distribution develops easily with a related increase in  $I_g$ . This results in the formation of banded structures.

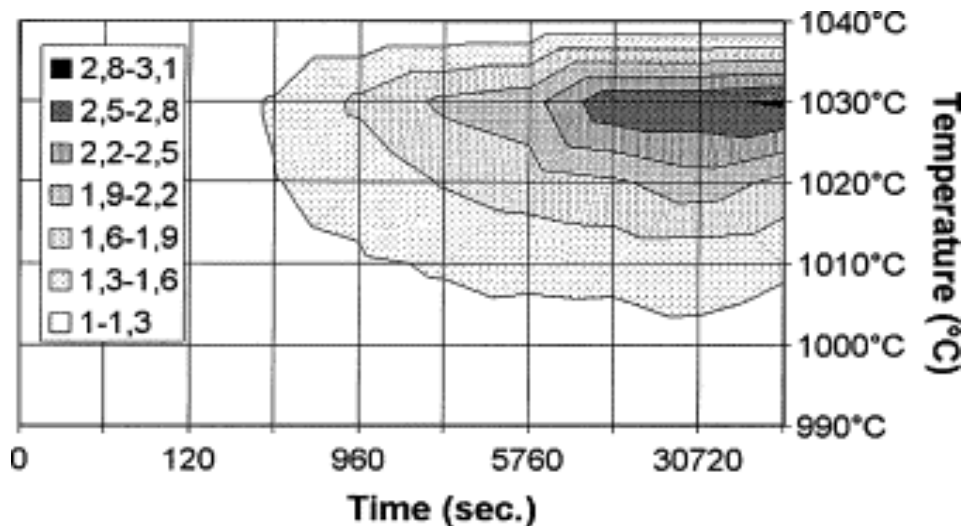


Fig. 14. Heterogeneity index map as a function of isothermal heat treating conditions.

These results may explain the good agreement between experimental data and simulations for short duration heat treatments in Fig. 9 and the discrepancy for the longer duration.

In order to apply this approach to industrial casting, it would be necessary to consider the changes in characteristic length period and amplitude of chemical heterogeneities. In practice, it could be valuable to simply consider the upper bound of chemical heterogeneities measured in a given casting. From this value, the highest difference in volume fraction of  $\delta$ -phase between interdendritic and dendritic zones may be evaluated and used to set the spatial distribution of delta precipitates entering the calculations. It would then be possible by computer simulation to define isothermal heat treating conditions avoiding the formation of a non-acceptable microstructure from a manufacturing point of view. This type of simulation might be further improved by using experimentally based relations giving the evolution of  $\delta$ -phase volume fraction as a function of time and niobium content. Further work and in particular in situ experiments would be needed to study these evolutions at a local level.

## 7. Conclusions

In this paper, grain growth has been simulated by the Monte-Carlo method by choosing initial simulation conditions in the process window for hot deformation of the Alloy 718 and was compared with experimental data. Results show that the Monte-Carlo method is a powerful tool to study the Zener pinning effect even for a heterogeneous distribution of particles. Results also show that a 2-D simulation is sufficient to describe a 3-D process like grain growth. This investigation has allowed to:

- assess the influence of several parameters during heat treatment like temperature, heat treating duration and fraction of second phase particles,
- propose a relationship between the Monte-Carlo step and the real time.

It is of practical interest in order to improve the capability to predict the microstructural evolution in a real wrought piece. Furthermore, it allows to know precisely the time when microstructural heterogeneities appear during heat treatment.

The present study is a part of an extensive work devoted to understanding the micro-mechanisms controlling the microstructural evolution in the nickel base superalloy 718. At present, an accurate model is developed in order to take into account the evolution of the precipitate fraction as a function of time, by using an algorithm coupling Monte-Carlo method and finite difference method. Therefore, the last parameter to study is the strain which is expected to have an influence on the kinetics of precipitation of the  $\delta$ -phase and on the grain boundary mobility.

## Acknowledgements

The authors would like to acknowledge Aubert & Duval Compagny, and the Région Midi-Pyrénées for providing materials and financial support for this study. Dr. D. Poquillon and Dr. J. Lacaze are also acknowledged for their fruitful and constructive contributions.

## References

- S. Coste, E. Andrieu and J. Huez, *Proceedings Matériaux 2002 Tours* (2002).
- M. Stockinger, E. Kozeschnick, B. Buchmayr and W. Horvath, *Proceedings Superalloys 718, 625, 706 and Various Derivatives*, TMS publication (2001), pp. 141–183.
- P.M. Hazzledine and R.D.J. Oldershaw, *Philos. Mag.* **A61** (1990), p. 579.
- J. Gao, R.G. Thompson and B.R. Patterson, *Acta Mater.* **45** (1997), p. 3653.
- D. Weygand, Y. Bréchet and J. Lépinoux, *Acta Mater.* **47** (1999), p. 961.
- B.K. Kad and P.M. Hazzledine, *Mater. Sci. Eng.* **A238** (1997), p. 70.
- D.J. Srolovitz, M.P. Anderson, G.S. Grest and P.S. Sahni, *Acta Metall.* **32** (1984), p. 1429.
- S. Ling and M.P. Anderson, *JOM* **9** (1992), p. 30.
- Y. Saito, *Mater. Sci. Eng.* **A223** (1997), p. 114.

Corresponding author. Tel.: +33 5 62 88 56 62; fax: +33 5 62 88 56 63.